absence of the field. This susceptibility enhancement points to coupling between polar ordering of dye molecules in the electric field and the uniaxial organization of the nematic solvent in a magnetic field. Additional evidence of this coupling is revealed in magnetically aligned samples by a more rapid rise of the second harmonic intensity with increasing temperature under the electric field. In an ideal system the magnetically aligned nematic alloy can be regarded as an "Ising-like" medium in which the nematic and external fields confine dipolar dye molecules along directions parallel or antiparallel to the electric field.

Acknowledgment. This project was funded by the U.S. Department of Energy through Grant No. DEFG02-91ER45439 to the University of Illinois Materials Research Laboratory. Partial funding in the early stages was also provided by 3M Co. We acknowledge J. Wu of our laboratory for the synthesis of the nematic polymer and Gary Boyd of 3M for helpful advice on the NLO experimental setup.

Appendix

The order parameter of the nematic solvent and the dissolved chromophore would be given by

$$S = \langle (3\cos^2\theta - 1)/2 \rangle = \int_0^\pi p(\theta)[(3\cos^2\theta - 1)/2] \sin\theta \, d\theta / \int_0^\pi p(\theta) \sin\theta \, d\theta \quad (14)$$

where θ is the angle of molecules with respect to the director axis, and $p(\theta)$ is the distribution function (Boltzmann distribution):

$$p(\theta) = \exp(-U(\theta)/kT) \quad (15)$$

where $U(\theta)$ is the potential energy of the dipole in the matrix. In a nematic matrix $U(\theta) = U'(\theta) - \mu E \cos\theta$, where $U'(\theta)$ is 0 in an isotropic medium and represents the local contribution of intermolecular interactions to the thermodynamic potential. In the Ising model, molecules are perfectly aligned, $\theta = 0$ or $\theta = \pi$, and $S = 1$, thus

$$\langle \cos^3\theta \rangle_{\text{Ising}} = \int_0^\pi p(\theta) \cos^3\theta \sin\theta \, d\theta / \int_0^\pi p(\theta) \sin\theta \, d\theta \quad (16)$$

$$= \int_0^\pi (\cos^3\theta) \exp(\mu E \cos\theta/kT) \times \exp(-U'(\theta)/kT) \sin\theta \, d\theta / \int_0^\pi \exp(\mu E \cos\theta/kT) \times \exp(-U'(\theta)/kT) \sin\theta \, d\theta \quad (17)$$

$$= \int_0^\pi (\cos^4\theta \mu E/kT + \ldots) \exp(-U'(\theta)/kT) \sin\theta \, d\theta / \int_0^\pi [1 + (\mu E \cos\theta/kT)^2/2 + \ldots] \times \exp(-U'(\theta)/kT) \sin\theta \, d\theta \quad (18)$$

The exponential functions are expanded and then reduced as follows. Keeping the first term in both expansion equations and neglecting the other terms for $\cos\theta = 1$ and $\mu E/kT \ll 1$

$$\langle \cos^3\theta \rangle_{\text{Ising}} = \int_0^\pi (\mu E/kT) \exp(-U'(\theta)/kT) \sin\theta \, d\theta / \int_0^\pi \exp(-U'(\theta)/kT) \sin\theta \, d\theta \quad (19)$$

Corrosion Reactions of $YBa_2Cu_3O_{7-x}$ and $Tl_2Ba_2Ca_2Cu_3O_{10+x}$ Superconductor Phases in Aqueous Environments

Ji-Ping Zhou and John T. McDevitt*

Department of Chemistry and Biochemistry, University of Texas at Austin, Austin, Texas 78712

Received November 20, 1991. Revised Manuscript Received March 24, 1992

The chemical reactions leading to the decomposition of superconducting $YBa_2Cu_3O_{7-x}$ ($0 > x > 0.05$) in water solution and water vapor at different temperatures were investigated and the corrosion products were characterized using X-ray diffraction and scanning electron microscopy. Although the $YBa_2Cu_3O_{7-x}$ phase is stable in some nonaqueous solvents, it reacts readily with water, acids, carbon dioxide, and carbon monoxide. Samples of $YBa_2Cu_3O_{7-x}$ soaked in water solution at 25, 50, and 75 °C all produce $BaCO_3$ and CuO corrosion products as determined by X-ray powder diffraction studies. Although there is some evidence for the formation of small amounts of Y_2BaCuO_5 and Y_2O_3, the majority of the Y-containing corrosion products are produced as amorphous phases. Our studies suggest that "Y_2BaCuO_5" is formed with a metastable or distorted structure. Moreover, when $YBa_2Cu_3O_{7-x}$ was exposed to water vapor equilibrated at a temperature of 75 °C, $BaCO_3$ forms and increases in amount with exposure time. On the other hand, CuO and "Y_2BaCuO_5" form only in the initial stages of corrosion. For comparison, superconducting $Tl_2Ba_2Ca_2Cu_3O_{10+x}$ was also investigated, and similar results were obtained. Details related to the corrosion of these two high-T_c phases are discussed herein.

Introduction

High-T_c phases $YBa_2Cu_3O_{7-x}$ and $Tl_2Ba_2Ca_2Cu_3O_{10+x}$ are p-type superconductors due to insertion of excess oxygen into the inactive layers.[1,2] Mixed valence $Cu^{2+/3+}$ states are present within the CuO_2 sheets in both structures,[3-6] giving rise to one of the necessary conditions to suppress

(1) Cava, R. J.; Batlogg, B.; van Dover, R. B.; Murphy, D. W.; Sunshine, S.; Siegrist, T.; Remeika, J. P.; Rietman, E. A.; Zahurak, S.; Espinosa, G. P. *Phys. Rev. Lett.* **1987**, *58*, 1676.

(2) Suzuki, T.; Nagoshi, M.; Fukuda, Y.; Syono, Y.; Kikuchi, M.; Kobayashi, N.; Tachiki, M. *Phys. Rev. B.* **1989**, *40*, 5184.

(3) Capponi, J. J.; Chailout, C.; Hewat, A. W.; Lijay, P.; Marezio, M.; Nguyen, N.; Raveau, B.; Sopubeyroux, J. L.; Tholence, J. L.; Tournier, R. *Europhys. Lett.* **1987**, *3*, 1301.

0897-4756/92/2804-0953$03.00/0

the long-range antiferromagnetic order and induce superconductivity.[7] The $YBa_2Cu_3O_{7-x}$ superconductor possesses an oxygen-deficient perovskite structure which can be described in terms of layers packed along the c axis in a Cu(1)O–BaO–Cu(2)O_2–Y–Cu(2)O_2–BaO–Cu(1)O sequence.[3,4] In $Tl_2Ba_2Ca_2Cu_3O_{10+x}$, the structure consists of active $Ca(CuO_2)$ layers where the superconducting electrons are thought to reside and inactive "rocksalt" Tl_2O_2 layers bounded by (001) planes of BaO.[5] This material has the layer sequence along the c axis of Tl_2O_{2+x}–BaO–CuO_2–Ca–CuO_2–BaO–Tl_2O_{2+x}.[8] It has become apparent that superconductivity in the oxide superconductors is strongly tied to the presence of highly oxidized copper states as well as active alkali components. Both of these features lend to these materials high chemical reactivity. Thus, the issues of surface reactivity and long-term environmental stability are particularly important.

The corrosion reactivity of high-T_c phases under various conditions has been studied by a number of authors utilizing a variety of different techniques. One of the first reports in this regard was by Rosamilia et al.,[9,10] who utilized electrochemical techniques to study reactions at $YBa_2Cu_3O_{7-x}$ surfaces. In the study they found that $YBa_2Cu_3O_7$ dissolves in aqueous acids, the dissolution rate is proportional to concentration of H^+ over the range of 2–100 mM and the reaction is controlled by mass transport of H^+ to the solid–liquid interface. Also, the formation of gas bubbles at the surface was ascribed to the evolution of oxygen. The following reaction was proposed to account for their observations:

$$Cu^{3+} + \tfrac{1}{2}H_2O \rightarrow H^+ + \tfrac{1}{4}O_2 + Cu^{2+} \quad (1)$$

However, the existence of Cu^{3+} species could not be detected by electrochemical methods. More recent studies conducted by mass spectrometry suggest that the source of the evolved oxygen is the superconductor lattice rather than the oxidation of water.[11] Rosamilia et al.[9,10] noted also that the decomposition of the $YBa_2Cu_3O_{7-x}$ lattice occurred commensurate with the leaching of Ba^{2+} ions into the water phase and that similar reactivity occurred with 1 M NaCl and 1 M $NaClO_4$. No appreciable amounts of Y or Cu ions were detected in any of the aqueous solutions. The following reaction was formulated to account for their observation:

$$YBa_2Cu_3O_7 + xH_2O \rightarrow 2Ba^{2+} + Cu_3YO_5 + (1 + x/2)O_2 + 2xH^+ + (4 + 2x)e^- \quad (2)$$

Other research groups have also examined the surface reactivity of high-T_c phases using electrochemical methods[12-16] and $La_{1.8}Sr_{12}CuO_4$, $YBa_2Cu_3O_{7-x}$, $Bi_2Sr_2CaCu_2O_{8+x}$ and $Tl_2Ba_2Ca_2Cu_3O_{10+x}$ have been studied in this regard. Much information about the surface chemistry of these materials has been gleaned from the use of cyclic voltammetric experiments recorded at epoxy-encapsulated superconductor electrode assemblies. In carefully dried nonaqueous solvent systems, these electrodes display reversible and reproducible voltammetry similar in behavior to that obtained at noble metal electrodes such as Pt or Au. However, the addition of small amounts of water to the electrolytic fluid leads to a drastic degradation in the performance of the ceramic electrode. Thus, monitoring the voltammetric response as a function of exposure time to corrosive media provides a very sensitive means to estimate the corrosion reactivity of high-T_c phases.[17] In fact, the three p-type superconductors, $YBa_2Cu_3O_{7-x}$, $Bi_2Sr_2CaCu_2O_{8+x}$, and $Tl_2Ba_2Ca_2Cu_3O_{10+x}$ all react with water[12,13,15-17] and have been studied by this method.

Bachtler et al.[18] reported that when $YBa_2Cu_3O_7$ electrodes are treated by anodic or cathodic polarization in aerated 0.1 M NaOH, white BaO or red-brown CuO precipitates collect on the porous surface of the electrodes. The precipitates were observed by scanning electron microscopy (SEM) and characterized by energy-dispersive spectroscopy (EDS) and X-ray photoelectron spectroscopy (XPS).

The most comprehensive work reported to date concerning the characterization of corrosion products of $YBa_2Cu_3O_{7-x}$ is that of Yan et al.,[19] who find that the material decomposes in the water to form CuO, $Ba(OH)_2$, and evolved oxygen gas. The $Ba(OH)_2$ is freely soluble in water and reacts with CO_2 to produce $BaCO_3$. The following two reactions summarize the reactivity:

$$2YBa_2Cu_3O_7 + 3H_2O \rightarrow Y_2BaCuO_5 + 3Ba(OH)_2 + 5CuO + \tfrac{1}{2}O_2 \quad (3)$$

$$Ba(OH)_2 + CO_2 \rightarrow BaCO_3 + H_2O \quad (4)$$

According to their study, X-ray powder diffraction studies revealed that after a 16-h treatment in water at 75 °C the composition of the residue consisted of CuO (~53%), $BaCO_3$ (~36%), and Y_2BaCuO_5 (~11%). Moreover, X-ray measurements of a sample treated in air at 85 °C with 85% relative humidity for 90 min showed some evidence of a very small amount of $Cu(OH)_2$ along with a relatively large fraction of surface-localized amorphous phase(s).

Similar experiments reported by Bansal and Sandkuhl[20] revealed that the degraded surface of the $YBa_2Cu_3O_{7-x}$ sample contained $BaCO_3$, CuO, and unreacted $YBa_2Cu_3O_{7-x}$ after the sample reacted with water solution in a closed system. However, in an open system, the corrosion products consisted of $BaCO_3$, CuO, Y_2BaCuO_5, and unreacted $YBa_2Cu_3O_{7-x}$. The authors speculated that the white precipitate of $BaCO_3$ which they observed on the

(4) David, W. I. F.; Harrison, W. T. A.; Gunn, J. M. F.; Moze, O.; Soper, A. K.; Day, P.; Jorgenson, J. D.; Capone II, D. W.; Schuller, I. K.; Seger, C. U.; Zhang, K.; Grace, J. D. *Nature* **1987**, *327*, 310.
(5) Cox, D. E.; Torardi, C. C.; Subramanian, M. A.; Gopalakrishnan, J.; Sleight, A. W. *Phys. Rev. B.* **1988**, *38*, 6624.
(6) Torardi, C. C.; Subramanian, M. A.; Calabrese, J. C.; Gopalakrishnan, J.; McCarron, E. M.; Morrissey, K. J.; Askew, T. R.; Flippen, R. B.; Chowdhry, U.; Sleight, A. W. *Phys. Rev. B* **1988**, *38*, 255.
(7) Manthiram, A.; Parathaman, M.; Goodenough, J. B. *Physica C* **1990**, *171*, 135.
(8) Manthiram, A.; Goodenough, J. B. *Appl. Phys. Lett.* **1988**, *53*, 420.
(9) Rosamilia, J. M.; Miller, B.; Scheemeyer, L. F.; Waszczak, J. V.; O'Bryan, H. M. Jr. *J. Am. Electrochem. Soc.* **1987**, *134*, 1863.
(10) Magee, V. M.; Rosamilia, J. M.; Kometani, T. Y.; Scheemeyer, L. F.; Waszczak, J. V.; Miller, B. *J. Electrochem. Soc.* **1988**, *135*, 3026.
(11) Salvador, P.; Fernandez-Sanchez, E.; Garcia Dominguez, J. A.; Amador, J.; Cascales, C.; Rasines, I. *Solid State Commun.* **1989**, *70*, 71.
(12) McDevitt, J. T.; Longmire, M.; Gollmar, R.; Jernigan, J. C.; Dalton, E. F.; McCarley, R.; Murray, R. W.; Little, W. A.; Yee, G. T.; Holcomb, M. F.; Hutchinson, J. E.; Collman, J. P. *J. Electroanal. Chem.* **1988**, *243*, 465.
(13) McDevitt, J. T.; McCarly, R. L.; Dalton, E. F.; Gollmar, R.; Murray, R. W.; Collman, J.; Yee, G. T.; Little, W. A. Symposium on Chemistry of High Temperature Superconductors II. American Chemical Society: Washington, DC, 1988; p 72.
(14) Rochani, S.; Hibbert, D. B.; Dou, S. X.; Bourdillon, A. J.; Liu, H. K.; Zhou, J. P.; Sorrell, C. C. *J. Electroanal. Chem.* **1988**, *248*, 461.
(15) Fleischer, N. A.; Manassen, J. *J. Electrochem. Soc.* **1988**, *135*, 3174.
(16) Gollmar, R. O.; McDevitt, J. T.; Murray, R. W.; Collman, J. P.; Yee, G. T.; Little, W. A. *J. Electrochem. Soc.* **1989**, *136*, 3696.
(17) Riley, D. R.; McDevitt, J. T. *J. Electroanal. Chem.* **1990**, *295*, 373.
(18) Bachtler, G. H.; Lorenz, W. J.; Schindler, W.; Saemann-Ischenko, G. *J. Electrochem. Soc.* **1988**, *135*, 2284.
(19) Yan, M. F.; Barns, R. L.; O'Bryan, H. M.; Gallagher, P. K.; Sherwood, R. C.; Jin, S. *Appl. Phys. Lett.* **1987**, *51*, 532.
(20) Bansal, N. P.; Sandkuhl, A. L. *Appl. Phys. Lett.* **1988**, *52*, 323.

surface of their sample was probably formed when the water solution was cooled to room temperature due to the lower solubility of $BaCO_3$ at this temperature.

The corrosion reactivity of $YBa_2Cu_3O_{7-x}$ at temperatures up to 1000 °C in wet carbon dioxide and carbon monoxide atmospheres has been reported by Gallagher and O'Bryan,[21] Zhang et al.,[22] and Gao et al.[23] Under such conditions, the following reactions are thought to occur:

$$2Cu^{3+} + 2O^{2-} + CO \rightarrow 2Cu^{2+} + (CO_3)^{2-} \quad (5)$$

$$O^{2-} + CO_2 \rightarrow (CO_3)^{2-} \quad (6)$$

According to these studies, barium carbonate and/or copper oxide are always present in the corroded phase assemblage;[21-23] however, the formation of crystalline yttrium compounds, including Y_2O_3, Y_2CuO_5, and Y_2BaCuO_5, is dependent upon the temperature and atmospheric conditions.[21,23]

In this paper, the corrosion reactivity of $YBa_2Cu_3O_{7-x}$ in water solution and water vapor at different temperatures is further described. Scanning electron microscopy and X-ray powder diffraction are utilized to characterize the details of the corrosion. The products of the corrosion and surface morphology of the degraded superconductor are discussed. For comparison purposes, the $Tl_2Ba_2Ca_2Cu_3O_{10}$ superconductor is also reported.

Experimental Section

Samples of nominal composition $YBa_2Cu_3O_{7-x}$ ($0 > x > 0.05$) were prepared by solid-state reaction of Y_2O_3, $BaCO_3$, and CuO at 935 °C in air for 6 h followed by annealing at 430 °C for 48 h in flowing oxygen. Samples of nominal composition $Tl_2Ba_2Ca_2Cu_3O_{10+x}$ were obtained by introducing into a preheated furnace at 900 °C the appropriate mixture of Tl_2O_3, BaO_2, CaO, and CuO pelletized and wrapped in a gold foil. The sample was presintered for 10 min in air and then quenched to liquid nitrogen temperature. The mixture was sintered at 900 °C for another 10 min in air after one intermittent grinding, pelletized, and then quenched into liquid nitrogen for a second time. Before and after characterization, all superconductor samples were stored in a desiccator.

The ceramic pellet samples (~14-mm diameter, 500 mg) were soaked in deionized water at 25, 50, and 75 °C for 2 days. The powder samples were prepared by grinding disks with an agate mortar and pestle for ~10 min, mixing 150 mg of powder with a few drops of acetone, and coating the powder onto a 25 mm × 30 mm glass slide. Samples of this type were exposed to water vapor that was equilibrated with the liquid at temperatures of 25, 50, and 75 °C. These materials were exposed to the water vapor for periods up to 30 h.

Before and after corrosion the samples were characterized by X-ray powder diffraction (XRD; Philips Electronic Instruments, Mount Vernon, New York) with Cu Kα radiation and by scanning electron microscopy (JEOL 35CF, JEOL, Ltd., Tokyo) equipped with energy-dispersive spectrometer (Model 8000, Kevex Instruments, San Carlos, CA). The microscope was operated at an accelerating voltage of 25 kV. The X-ray diffraction samples were prepared in the same way as the glass slide sample, using the dried corrosion products.

Oxygen content of $YBa_2Cu_3O_{7-x}$ samples was characterized by iodometric titrations.[24,25] Transition temperatures of the samples prior to corrosion were determined using standard four-point probe resistivity measurements.

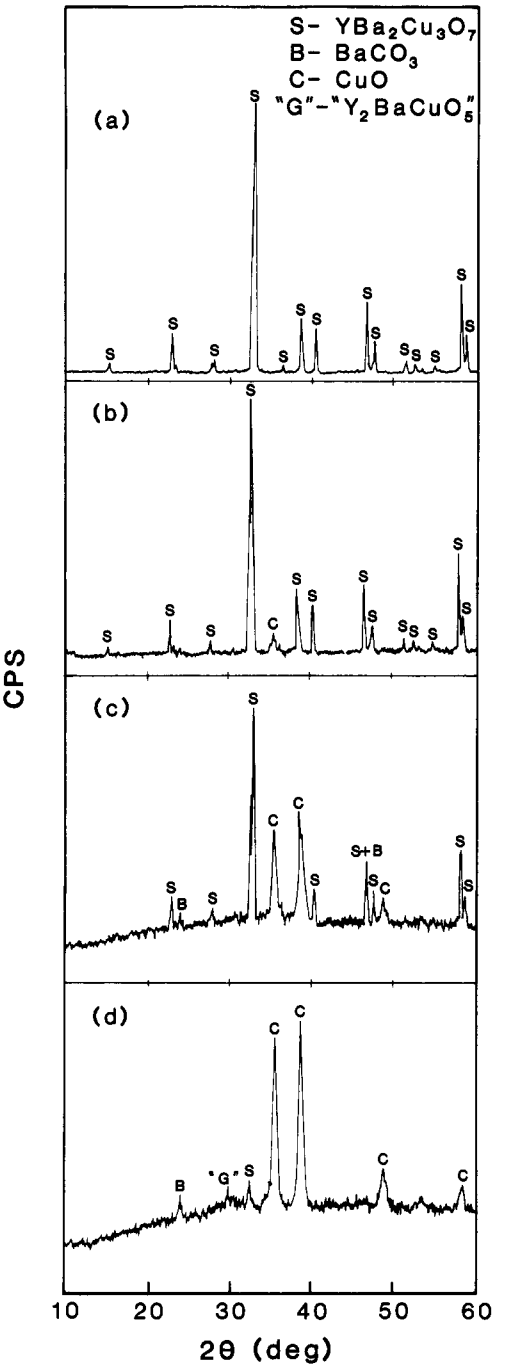

Figure 1. XRD patterns of ceramic pellets of $YBa_2Cu_3O_{7-x}$ that were soaked in water for 2 days at different temperatures: (a) $YBa_2Cu_3O_{7-x}$ before corrosion, (b) soaked in water held at 25 °C, (c) at 50 °C, and (d) at 75 °C.

Results and Discussion

Powder diffraction data for samples of $YBa_2Cu_3O_{7-x}$ exposed to water solution for 2 days at temperatures of 25, 50, and 75 °C are illustrated in Figure 1. For comparison purposes, data acquired prior to any water exposure is also provided (Figure 1a). Accordingly, CuO, $BaCO_3$, and Y_2BaCuO_5 phases are not detected in the original $YBa_2Cu_3O_{7-x}$ samples. However, after the samples are exposed to water solution, CuO and $BaCO_3$ phases appear in the samples (Figure 1b–d) with the former being the predominant product. The relative intensity of all the diffraction signals decreases dramatically as the corrosion reaction proceeds. The effect can be attributed to the formation of amorphous corrosion phases which collect on the surface of the degraded sample as has been noted

(21) Gallagher, P. K.; Grader, G. S.; O'Bryan, H. M. Jr. *Mater. Res. Bull.* **1988**, *23*, 1491.
(22) Zhang, L.; Chen, J.; Chan, H. M.; Harmer, M. P. *J. Am. Ceram. Soc.* **1989**, *72*, 1997.
(23) Gao, Y.; Merkle, K. L.; Zhang, C.; Balachandran, U.; Poeppel, R. *J. Mater. Res.* **1990**, *5*, 1363.
(24) Manthiram, A.; Swinnea, J. S.; Sui, Z. T.; Steinfink, H.; Goodenough, J. B. *J. Am. Chem. Soc.* **1987**, *109*, 6667.
(25) Parathaman., M.; Mathiram, A.; Goodenough, J. B. *J Solid State Chem.* **1990**, *87*, 479.

Table I. XRD Results for the Corrosion of $YBa_2Cu_3O_{7-x}$ in Water Solution

	estimated phase contents,[a] wt%				
T, °C	$YBa_2Cu_3O_{7-x}$	$BaCO_3$	"Y_2BaCuO_5"	CuO	amorphous phase(s)[b]
25	47[c]			5	48
50	34	2		13	51
75	5	4	4	22	65

[a] The following steps were utilized to estimate the phase contents for the corroded high-T_c samples: A series of $YBa_2Cu_3O_{7-x}$, $BaCO_3$, Y_2BaCuO_5, and CuO specimens were synthesized in phase-pure form. Mixtures of these four component phases were prepared and examined by XRD to establish the relative scattering efficiency for each phase. By comparing the most intense diffraction line for each identified phase with the maximum intensity of $YBa_2Cu_3O_{7-x}$ before corrosion, the relative contents of the different phases were obtained. [b] Amorphous phase(s) contents were calculated by subtracting the sum of the $YBa_2Cu_3O_{7-x}$, $BaCO_3$, "Y_2BaCuO_5", and CuO phase contents from 100%. [c] Before corrosion the number of counts for the most intense peak for $YBa_2Cu_3O_{7-x}$ was 4916.

previously by other authors.[19] Careful inspection of the diffraction data reveals that a Y_2BaCuO_5 like species is present on the surface of the corroded sample. The phase displays some, but not all, of the diffraction peaks that normally are associated with authentic Y_2BaCuO_5 samples.[26] In this regard, only one line of the "Y_2BaCuO_5" phase (d spacing of this line varies from 0.2981 to 0.3077 nm) can be considered to be consistent with the authentic pattern of Y_2BaCuO_5. Two other lines more closely match the literature data for Y_2O_3. Thus, the "Y_2BaCuO_5" phase which appears during the decomposition of the high-T_c phase may arise from a distortion of the $YBa_2Cu_3O_{7-x}$ lattice which occurs during the early stages of corrosion. Also, at the initial stages of corrosion there is a green coloration of the surface of the corroded sample consistent with the presence of Y_2BaCuO_5 phase. However, the inconsistent diffraction data lead us to believe that the product is formed as a "metastable Y_2BaCuO_5". After prolonged exposure to water, the diffraction signals for the "Y_2BaCuO_5" peaks are totally lost along with the green color.

From the data presented in Figure 1, it is apparent that the rate of corrosion of $YBa_2Cu_3O_{7-x}$ is dramatically dependent upon the temperature. Additional data concerning the surface composition after water solution treatment are provided in Table I. After 2 days at 25 °C, there is only a slight degradation of the superconductor surface, whereas the sample held at 50 °C shows substantial evidence for corrosion, and the specimen exposed at 75 °C is almost completely degraded. In fact, after the exposure at 75 °C the sample is broken into several small pieces. However, in spite of the fact that higher temperatures promote more rapid decomposition of $YBa_2Cu_3O_{7-x}$ lattice, more $BaCO_3$ crystals precipitate onto the surface of the ceramic sample at low temperatures. Accordingly, the precipitation of $BaCO_3$ from water is dependent upon the variable solubility of this compound: 0.002 g/100 mL at 20 °C and 0.0065 g/100 mL at 100 °C.[27]

Figure 2 shows the surface morphology of $YBa_2Cu_3O_{7-x}$ ceramic pellets after soaking in water at 50 °C for 2 days as revealed by scanning electron microscopy. In Figure 2a, the sample is removed from the solution and the excess water on the surface of the pellet is allowed to evaporate. In Figure 2b the excess water is removed immediately by washing with acetone upon extraction of the sample from the solution. In both SEM micrographs the presence of white needles of the $BaCO_3$ phase is readily apparent. There are, however, dramatic differences between the morphologies of the two samples. For the former sample (Figure 2a), some of the water soluble corrosion products are forced to precipitate onto the surface of the pellet in a relatively rapid fashion. Under such conditions, a thick crust of $BaCO_3$ forms which covers the entire surface of the sample. On the other hand, the surface of the latter sample (Figure 2b) possesses fine $BaCO_3$ needles which form rather slowly thereby decorating only selected regions of the surface of the ceramic.

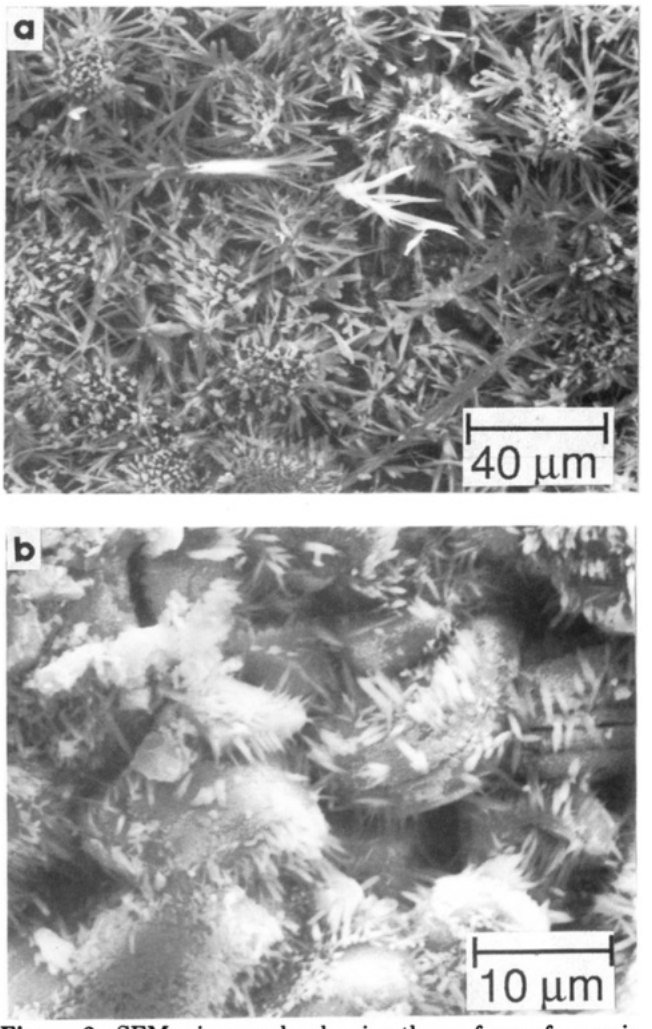

Figure 2. SEM micrographs showing the surfaces of ceramic pellets of $YBa_2Cu_3O_{7-x}$ that were soaked in water at 50 °C for 2 days, (a) sample was removed from water and the excess water was allowed to evaporate from the sample, (b) upon removal of sample, the excess water was removed immediately with an acetone wash.

To further explore the reactivity of $YBa_2Cu_3O_{7-x}$ with water, powders of the ceramic superconductor were exposed to water vapor equilibrated at 25, 50, and 75 °C. Similar to the solution-phase measurements, the temperature of the vapor plays a predominant role in determining the kinetics and dynamics of the degradation of the high-T_c material. X-ray diffraction data for powders exposed to 75 °C water vapor for times ranging from 5 to 30 h are illustrated in Figure 3, and phase contents for such samples are summarized in Table II. Under such conditions there is a monotonic decrease in the $YBa_2Cu_3O_{7-x}$ content com-

(26) Steinfink, H.; Swinnea, J. S.; Sui, Z. T.; Hsu, H. M.; Goodenough, J. B. *J. Am. Chem. Soc.* **1987**, *109*, 3348.

(27) Weast, R. C.; Lide, D. R.; Astle, M. J.; Beyer, W. H. *CRC Handbook of Chemistry and Physics*; CRC Press, Inc.: Boca Raton, FL, 1989–1990.

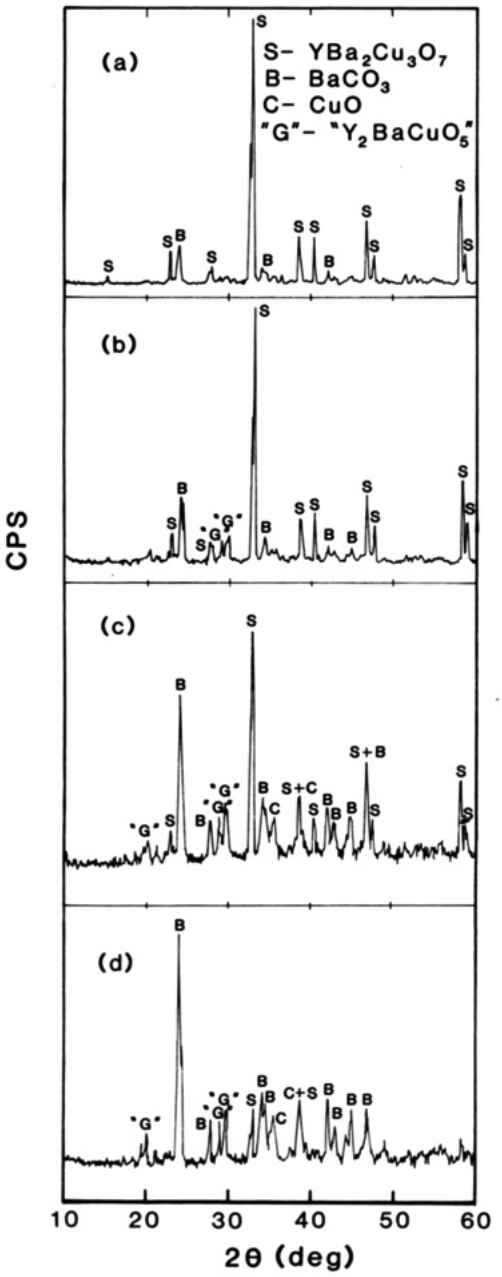

Figure 3. XRD pattern $YBa_2Cu_3O_{7-x}$ powder samples exposed to water vapor equilibrated at 75 °C for (a) 5, (b) 10, (c) 20, and (d) 30 h.

Table II. XRD Results for the Corrosion of $YBa_2Cu_3O_{7-x}$ in Water Vapor

time, h	estimated phase contents,[a] wt %				
	$YBa_2Cu_3O_{7-x}$	$BaCO_3$	"Y_2BaCuO_5"	CuO	amorphous phase(s)
0	100				0
5	69	9			22
10	47	11	4		38
20	18	13	4	5	60
30	3	19	5	5	68

[a] Phase contents were estimated according to the procedure described in the caption for Table I.

mensurate with a monotonic increase in $BaCO_3$ content with exposure time. For the "Y_2BaCuO_5" and CuO phases there is an induction period before these products are detected and, soon thereafter, their relative phase contents remain constant. Moreover, whereas for the solution-phase degradation CuO is the dominant corrosion product, $BaCO_3$ is the major phase for the water vapor condition.

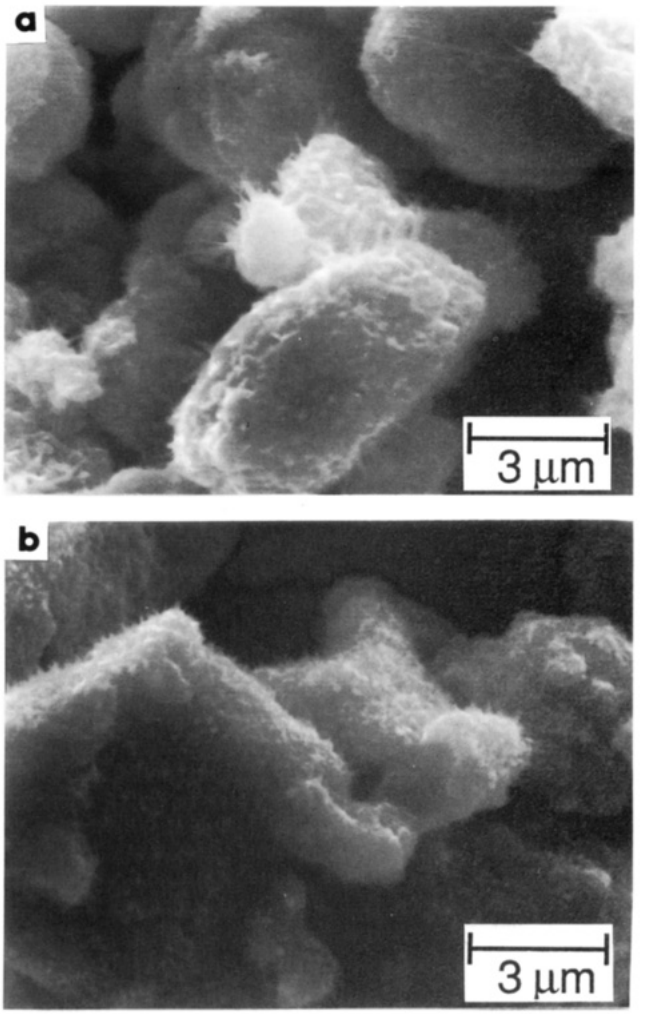

Figure 4. SEM micrographs of the $YBa_2Cu_3O_{7-x}$ powder samples exposed to water vapor equilibrated at 75 °C for (a) 15 and (b) 30 h.

An important difference between the solution- and vapor-phase corrosion experiments is that for the former it is possible for the individual metal ions to selectively leach away from the surface of the corroding material thereby changing the stoichiometry of the sample. In contrast the conditions for the vapor phase are such that the metal ion stoichiometry remains constant. The difference becomes apparent when comparing the phase contents of the $YBa_2Cu_3O_{7-x}$ corrosion products after long exposure times to water solution and to water vapor. Exhaustive corrosion of $YBa_2Cu_3O_{7-x}$ in solution produces 12.5% $BaCO_3$, 12.5% "Y_2BaCuO_5", and 75% CuO whereas for the vapor 65% $BaCO_3$, 17.5% "Y_2BaCuO_5", and 17.5% CuO are obtained. The theoretical values for the stoichiometric decomposition of the $YBa_2Cu_3O_7$ phase according to eqs 3 and 4 are 40.9% $BaCO_3$, 31.7% Y_2BaCuO_5, and 27.4% CuO. As expected, there is better agreement between the ideal stoichiometries and those obtained in the vapor phase than those for the solution-phase experiments. The low $BaCO_3$ content for the solution measurements can be attributed to the leaching of $Ba(OH)_2$ from the superconductor (eq 3). Energy dispersive spectroscopy (EDS) measurements reveal that water soaked $YBa_2Cu_3O_{7-x}$ samples are Ba deficient. Moreover, analysis of the water soluble residue shows the presence of large amounts of Ba compounds, and no detectable Cu or Y signal. Differences between the vapor phase and the theoretical values can be attributed to either phase segregation of the corrosion products onto the surface of the corroding sample and/or to the forma-

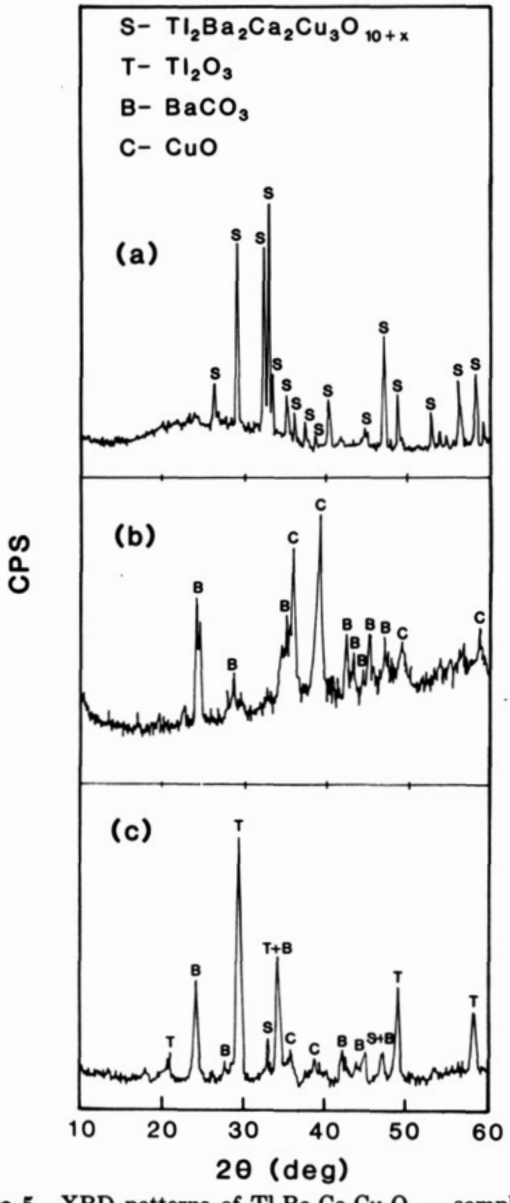

Figure 5. XRD patterns of $Tl_2Ba_2Ca_2Cu_3O_{10+x}$ samples (a) powder before corrosion (b) pellet soaked in water at 25 °C for 7 days and (c) powder exposed to water vapor equilibrated at 75 °C for 2 days.

tion of amorphous corrosion products which are not detected by the diffraction method. Consistent with the latter possibility is the fact that there is a systematic decrease in the diffraction intensity as the corrosion proceeds.

Figure 4 illustrates electron micrographs of $YBa_2Cu_3O_{7-x}$ powders after 15- and 30-h exposure to water vapor equilibrated at 75 °C. The $BaCO_3$, "Y_2BaCuO_5", CuO, and amorphous corrosion products uniformly coat the surface of the superconductor with an insulating sheath. Under these conditions, the physical appearance of the surface layer does not change to any great extent as the corrosion reactions proceed.

As stated above, one advantage of the vapor-phase corrosion method is that the metal cations in the corrosion products maintain their stoichiometric ratio. From a knowledge of the reaction scheme (i.e., eqs 3 and 4), it is apparent that a weight increase in the sample is expected as one mole of $YBa_2Cu_3O_7$ (formula weight 666.2 g) corrodes into $^5/_2$ mol of CuO, $^1/_2$ mol of Y_2BaCuO_5, and $^3/_2$ moles of $BaCO_3$ (combined factional formula weights = 724.2 g). Incorporation of atmospheric CO_2 into the corrosion products is responsible for the majority of the weight

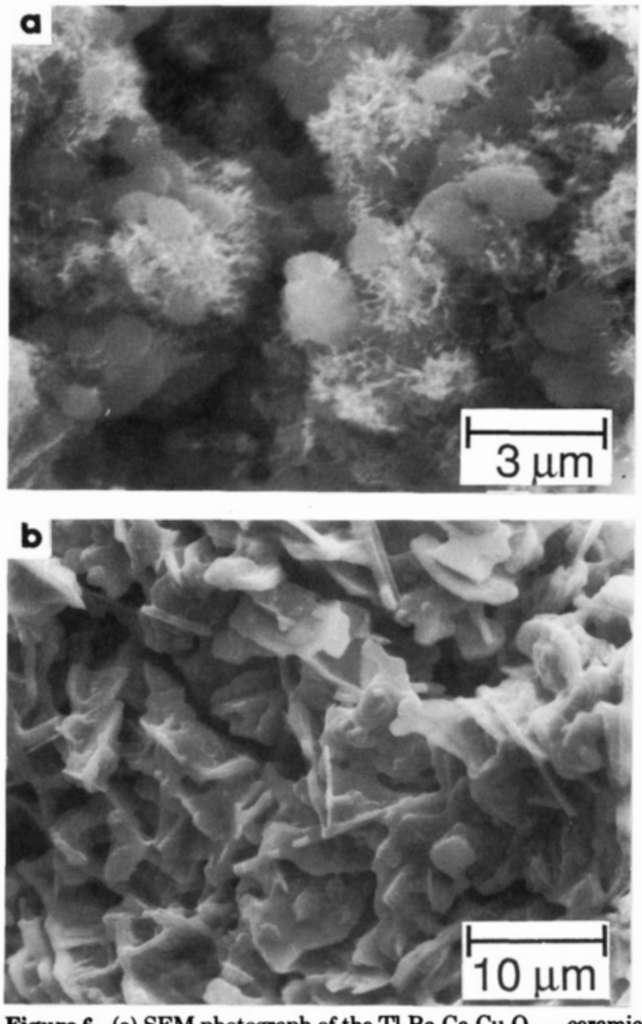

Figure 6. (a) SEM photograph of the $Tl_2Ba_2Ca_2Cu_3O_{10+x}$ ceramic pellet sample corroded by soaking in water at 25 °C for 7 days. The white needles which decorate the surface are $BaCO_3$ crystals which precipitated from the aqueous phase. (b) For comparison purposes, the sample is shown before exposure to water.

increase. Thus, a gravimetric study was conducted on $YBa_2Cu_3O_7$ powder exposed to water vapor over a period of 30 h. The data reveal that the corrosion reactions can be followed by this method and that rate proceeds rather smoothly suggesting that no passivating layer forms during the corrosion.

In addition to the degradation of $YBa_2Cu_3O_{7-x}$, the corrosion of $Tl_2Ba_2Ca_2Cu_3O_{10+x}$ was also studied. To successfully complete these studies, more aggressive (i.e., longer reaction times) were employed. Figure 5a displays the XRD pattern for $Tl_2Ba_2Ca_2Cu_3O_{10+x}$ before corrosion, Figure 5b after soaking a pellet in water solution for 7 days, and Figure 5c after exposure of powder to water vapor equilibrated at 75 °C for 2 days. The sample soaked in water solution yields CuO as the major corrosion product along with a small amount of $BaCO_3$. For this sample, Tl_2O_3 is not observed. On the other hand, for the vapor-phase experiment, Tl_2O_3, $BaCO_3$, and CuO are obtained; Tl_2O_3 and $BaCO_3$ are the major phases. Although no $CaCO_3$ is detected in the present work, previous authors have identified its presence in studies of other p-type superconducting materials after long exposure times.[28] The formation of $CaCO_3$ may depend upon the exposure conditions. EDS measurements of the water-soluble residue

(28) Golden, M. S.; Egdell, R. G.; Flavell, W. R. *J. Mater. Chem.* **1991**, *1*, 489.

reveal large amounts of Ba and Tl, trace amounts of Ca, and no detectable Cu. Figure 6 displays electron micrographs of $Tl_2Ba_2Ca_2Cu_3O_{10+x}$ samples before and after soaking in water solution for 7 days. The formation of $BaCO_3$ needles is noted in this superconductor phases also. Thus, the corrosion reactivity of $Tl_2Ba_2Ca_2Cu_3O_{10+x}$ displays many similarities to those observed for $YBa_2Cu_3O_{7-x}$.

In addition to the high intrinsic reactivity associated with the cuprate materials, surface microstructure factors such as grain boundaries, microcracks, and surface porosity are likely to play important roles in the decomposition of these compounds. To explore the relative importance of these factors, a series of five $YBa_2Cu_3O_{7-x}$ ceramic samples with densities ranging from 65 to 99% were prepared, and their relative reactivity with water was assessed. Interestingly, we find that there is not a large difference in the decomposition rates exhibited by the different specimens. Moreover, there is a definite trend for the lower density samples to be more stable than the higher density specimens. We conclude that the higher temperature utilized to prepare the high-density samples leads to the partial degradation of the high-T_c phase. The presence of these impurities serves to catalyze the decomposition of the lattice.[29] Thus, surface microstructure does not appear to be the dominating factor responsible for the high degradation rate of this material.

Conclusions

Cuprate superconductor phases react rapidly with water solution and vapor at low temperatures to revert back, at least partially, to metal oxide and carbonate salts from which they were initially formed. Moreover, some fraction of the high-T_c lattice decomposes to produce metastable and noncrystalline decomposition products. The formation of such materials is not surprising given that corrosion at low temperatures does not afford the possibility for the high ionic mobility necessary to form complex decomposition products. The complex oxide degradation products that do form likely display structural similarities to the host lattice. From the present studies, no appreciable amounts of Y- or Ca-containing corrosion products were identified. Only small amounts of metastable "Y_2BaCuO_5" were found in the initial stages of corrosion, disappearing after prolonged exposure times to water. Thus, for the low-temperature decomposition of the cuprate materials, kinetic factors and reaction conditions play dominant roles in determining the nature of the decomposition. For samples soaked in water, corrosion products become distributed between the solution and solid phases. Water solubility of the corrosion products play an important role determining the relative product distribution between the two phases. The Ba and Tl products tend to leach readily into water solution. On the contrary, reactions occurring in the presence the water vapor preserve the initial ion ratios simplifying the analysis of the corrosion product assemblage. Under such conditions, crystalline $BaCO_3$ and Tl_2O_3 degradation products form on the surface of the decomposed high-T_c samples and are readily detected by XRD. Thus, the corrosion product distribution for water solution and vapor conditions differ due to leaching effects which occur for liquid-phase corrosion. Finally, we note that ceramic samples of $YBa_2Cu_3O_{7-x}$ phase appear to degrade at least 3 times more rapidly than $Tl_2Ba_2Ca_2Cu_3O_{10+x}$. The enhanced reactivity for the former material observed herein occurs in spite of the fact that $YBa_2Cu_3O_{7-x}$ can be prepared in higher purity and with higher density.

Acknowledgment. This research was supported by the National Science Foundation, Grant No. DMR-8914476, by the National Association of Corrosion Engineers, and by the Welch Foundation. We thank Dr. J. B. Goodenough, Dr. M. Schmerling, Dr. M. Paranthaman, Dr. A. Manthiram, Dr. A. DeLozzane, and Dr. J. S. Swinnea for use of their facilities and helpful discussions. We also wish to thank Anna Grassini for proofing the manuscript.

Registry No. $YBa_2Cu_3O_{7-x}$, 123744-36-5; $BaCO_3$, 513-77-9; CuO, 1317-38-0; Tl_2O_3, 1314-32-5.

(29) The amounts of any impurities formed during the high-temperature synthesis of the dense samples were below the detection limits of X-ray powder diffraction.